Life History Traits Impact the Nuclear Rate of Substitution but Not the Mitochondrial Rate in Isopods

Nathanaëlle Saclier,*[,1] Clémentine M. François,[1] Lara Konecny-Dupré,[1] Nicolas Lartillot,[2] Laurent Guéguen,[2] Laurent Duret,[2] Florian Malard,[1] Christophe J. Douady,[1,3] and Tristan Lefébure*[,1]

[1]Univ Lyon, Université Claude Bernard Lyon 1, CNRS UMR 5023, ENTPE, Laboratoire d'Ecologie des Hydrosystèmes Naturels et Anthropisés, Villeurbanne, France

[2]Univ Lyon, Université Claude Bernard Lyon 1, CNRS UMR 5558, Laboratoire de Biométrie et Biologie Evolutive, Villeurbanne, France

[3]Institut Universitaire de France, Paris, France

***Corresponding authors:** E-mails: nathanaelle.saclier@univ-lyon1.fr; tristan.lefebure@univ-lyon1.fr.

Associate editor: Keith Crandall

Abstract

The rate of molecular evolution varies widely among species. Life history traits (LHTs) have been proposed as a major driver of these variations. However, the relative contribution of each trait is poorly understood. Here, we test the influence of metabolic rate (MR), longevity, and generation time (GT) on the nuclear and mitochondrial synonymous substitution rates using a group of isopod species that have made multiple independent transitions to subterranean environments. Subterranean species have repeatedly evolved a lower MR, a longer lifespan and a longer GT. We assembled the nuclear transcriptomes and the mitochondrial genomes of 13 pairs of closely related isopods, each pair composed of one surface and one subterranean species. We found that subterranean species have a lower rate of nuclear synonymous substitution than surface species whereas the mitochondrial rate remained unchanged. We propose that this decoupling between nuclear and mitochondrial rates comes from different DNA replication processes in these two compartments. In isopods, the nuclear rate is probably tightly controlled by GT alone. In contrast, mitochondrial genomes appear to replicate and mutate at a rate independent of LHTs. These results are incongruent with previous studies, which were mostly devoted to vertebrates. We suggest that this incongruence can be explained by developmental differences between animal clades, with a quiescent period during female gametogenesis in mammals and birds which imposes a nuclear and mitochondrial rate coupling, as opposed to the continuous gametogenesis observed in most arthropods.

Key words: **substitution rate, longevity, generation time, isopods.**

Introduction

The rate at which DNA accumulates substitutions varies widely among lineages (Lynch 2010; Bromham et al. 2015; Allio et al. 2017). Correlations have been observed between many life history traits (LHTs) and the rate of substitution, to the point that one could use ancestral rate reconstruction based on phylogenetic methods to infer ancestral LHTs (Lartillot and Delsuc 2012; Wu et al. 2017). Nevertheless, the mechanism at the origin of these correlations and the question of their universality remain unclear (Caccone et al. 2004; Baer et al. 2007; Allio et al. 2017).

Two broad categories of hypotheses have been proposed to explain the link between LHT and the rate of molecular evolution: hypotheses where the substitution rate depends on the DNA replication rate and hypotheses where it is controlled by the activity of the mitochondrial respiratory chain. In the first category, a well-established hypothesis is the generation time (GT) hypothesis (Li et al. 1987) which proposes that a species with shorter GT copies its genome more often per time unit, thereby accumulating more DNA replication errors. Correlations between GT and substitution rate have been observed in mammals (Ohta 1993; Bromham et al. 1996), birds (Mooers and Harvey 1994), protostomians (Thomas et al. 2010), and plants (Smith and Donoghue 2008). Hypotheses belonging to the second category rely on the assumption that the mitochondrial respiratory chain generates mutagenic reactive oxygen species (ROS). As a consequence species that generate more ROS are expected to accumulate more DNA damage, and in particular damage to the mitochondrial genome (Barja 2002). Two influences—one direct and one indirect—of mitochondrial respiratory chain activity on the substitution rate have then been proposed. First, species with high metabolic rate (MR) produce more ROS, accumulate more DNA damage, and so should have a higher substitution rate. Indeed, some studies have reported a correlation between MR and substitution rate (Martin et al. 1992; Gillooly et al. 2005). Second, Nabholz et al. (2008) proposed that mitochondrial mutations will be differentially counter-selected depending on the species longevity. The mitochondrial theory of aging proposes that mutations in the mitochondrial genome lead to a chain reaction by affecting the efficiency of the respiratory chain, thus leading to an increase in the production of ROS and a

correlative acceleration of aging (Kujoth et al. 2007). To counteract this effect and ultimately delay aging, selection is expected to act in long-lived species to reduce the mitochondrial mutation rate. One expected outcome of this indirect effect is a negative correlation between substitution rate and longevity. These two last hypotheses imply a direct causal link between the MR, the production of ROS and ultimately the mutation rate. Several studies have challenged the link between MR and ROS production (Barja 2007) but also the ROS influence on the mitochondrial mutation rate (Larsson 2010; Kennedy et al. 2013). While the former category of hypotheses (the DNA replication rate hypotheses) extends to all organelles and their genomes, the second set (the mitochondrial respiratory chain hypotheses) mostly applies to the mitochondrial genome (Galtier, Jobson, et al. 2009), as ROS are produced in the mitochondria where they directly induce damage to the mitochondrial genome. Using experimental mutagenesis on rat's mitonchondria, Richter et al. (1988) showed that mutations induced by ROS are 16 times more frequent in the mitochondrial genome than the nuclear genome.

While these questions are not new, we still lack a clear understanding of why substitution rates are not clock-like across taxa and which traits, if any, are responsible for the violation of a strict molecular clock. Trait covariation, a focus on a very restricted set of taxa, and a reduced number of studied loci, mostly mitochondrial, are but a few roadblocks preventing a better understanding of these questions, as we discuss below. First, disentangling the influence of different biological traits on the substitution rate is complicated by rampant trait covariation. In particular, GT, MR, and longevity are often strongly correlated along the slow-fast life history continuum (Jeschke and Kokko 2009). Second, most studies have been devoted to mammals and birds, two endothermic groups of amniotes, which calls into question the universality of the observed patterns and proposed hypotheses. Third, most studies are also based on few loci (most between one to six genes, with a few reaching 15 genes). Within a genome, substitution rates vary extensively due to variation in mutation rate (Wolfe et al. 1989; Ellegren et al. 2003) or selection pressure (Duret and Mouchiroud 2000) along the chromosomes. Estimates of rate variation could be further blurred by this intragenomic variation, in particular when a small number of loci are considered. Finally, most studies are based on mitochondrial genes (though there are exceptions, see Caccone et al. 2004; Nikolaev et al. 2007; Welch et al. 2008; Lartillot and Delsuc 2012). The mitochondrial genome has a very distinct evolutionary dynamic compared with the nuclear genome. Because it is maternally inherited, haploid, and has specific mutational exposure, repair mechanisms and replication machineries, the mitochondrial genome evolves under a very different effective population size, and at different mutation and recombination rates. As such, the usage of the mitochondrial genome as a marker to infer population histories and divergences is debated (Galtier, Nabholz, et al. 2009; Allio et al. 2017). At the very least, substitution rate variation observed in the context of the mitochondrial genome should not be generalized to the nuclear genome. To sum up, the respective influence of LHT on the nuclear and mitochondrial substitution rates requires further investigation.

In this study, we used the transition to the subterranean habitat to disentangle the influence of the replication rate and the activity of the mitochondrial respiratory chain on the mitochondrial and nuclear substitution rates. We used the unique features of the aquatic isopods of the Asellidae family: within this family, many species have independently become subterranean, offering an opportunity to study independent replicates of the same evolutionary transition from surface to groundwater habitats. This transition triggered an important modification of the LHT of the underground species, including an extension of their lifetime (5–10 times), a delay of sexual maturity and a decrease in the number of offspring (Henry 1976). As a response to food scarcity, subterranean organisms also tend to display low MRs (Hüppop 1987; Renault et al. 2002). Thanks to recent phylogenetic (Morvan et al. 2013) and genomic (Francois et al. 2016; Lefébure et al. 2017) studies, the phylogeny of Asellidae is now well-resolved and many nuclear genes have been sequenced for 13 independent surface/subterranean species pairs. We complemented these nuclear data sets with mitochondrial genome assemblies and tested the predictions of the DNA replication rate and mitochondrial respiratory chain hypotheses. Namely, if the activity of the mitochondrial respiratory chain is the main driver of change to the substitution rate, we expect a lower mitochondrial rate in the long-lived and low-metabolism subterranean species with little to no variation on the nuclear rate. Conversely, if the DNA replication rate is a major factor, we this time expect a decrease of the substitution rate in subterranean species that is of the same amplitude in the mitochondrial and nuclear genomes.

Results

Nuclear and Mitochondrial Data Set

For 13 pairs of surface and subterranean species, 386 one-to-one nuclear orthologous gene family alignments were taken from a previous study (Francois et al. 2016). Four gene families displaying evidence of contamination were discarded. A phylogeny of the 26 species was built with PhyML v3.0 (Guindon et al. 2010) by using the 382 nuclear genes. Except for two nodes with values at 97.4% and 98%, all nodes have a bootstrap value of 100% (supplementary fig. S1, Supplementary Material online). Nearly complete mitochondrial genomes for these 13 species pairs were de novo assembled using a combination of genomic and RNA-seq reads. Only the control region consistently failed to be assembled. The de novo mitochondrial genomes are syntenous and display the same gene order as the one already described in Asellidae and in the more distantly related isopod Oniscidea (Kilpert and Podsiadlowski 2006; Kilpert et al. 2012). Difficulty in assembling the mitochondrial control region in isopods is a well-known problem that has been interpreted as the result of an atypical mtDNA composed of linear monomers associated with circular "head-to-head" dimers (Raimond et al. 1999; Doublet et al. 2012). Twelve of the 13 mitochondrial protein coding genes (*atp8* was too small to be identified with

certainty) were identified for each species and their DNA sequences were concatenated and used to estimate a global mitochondrial substitution rate.

Effect of the Transition to Subterranean Habitat on Substitution Rates

For each of the 26 species, we computed a rate of synonymous substitution (d_S) per unit of time using the Bayesian software program CoEvol (Lartillot and Poujol 2012) independently for the nuclear (382 genes) and for the mitochondrial concatenations (12 genes, supplementary table S1, Supplementary Material online). If we ignore selection for codon usage, a transcriptome-wide d_S is expected to give a good estimate of the mutation rate. Correlations between the rate of molecular evolution and habitat were tested using PGLS (Phylogenetic Least Square) models. Moreover, inside each pair of species, we computed the posterior probability of an increase of the d_S in surface species (later names pp) as the frequency of samples from the CoEvol Monte-Carlo chain where the surface species has a higher d_S than the subterranean species. In the nuclear compartment, the d_S was significantly lower in subterranean species (PGLS, table 1, fig. 1), with a significant subterranean d_S decrease in 10 pairs out of 13 (fig. 1, pp > 0.90). However, in the mitochondrial genome, we observed no effect of the ecological status on the d_S (PGLS, table 1) with only one pair supporting an increase in d_S in the subterranean species (pp $= 1$), another supporting a decrease (pp $= 0$), and the remaining 11 pairs showing no significant d_S variation ($0.10 <$ pp < 0.90, fig. 1). To quantify the apparent decoupling between the mitochondrial and nuclear rates, we estimated the ratio of mitochondrial d_S to nuclear d_S ($d_{S_{mito}}/d_{S_{nucl}}$). Mitochondrial genes undergo a synonymous substitution rate 15.71 times faster than the nuclear genes but with some substantial variation across taxa (from 2.5× to 34.9×, supplementary table S2, Supplementary Material online). The variation in $d_{S_{mito}}/d_{S_{nucl}}$ was mostly explained by the nuclear contribution, with a mitochondrial d_S much more stable than the nuclear d_S (coefficient of variation of 8.96% against 51.67% in the mitochondrial and nuclear genome, respectively).

Impact of the Colonization Time

The comparative analysis presented in the last section, based on surface/subterranean independent species pair and using the present day ecological status in a regression model, implicitly amounts to assuming that the speciation event between the two species and the ecological transition are concomitant. However, in reality, speciation might have occurred long before the ecological transition. Some subterranean species have intermediate traits (microphthalmy, partial depigmentation) suggesting that they colonized the subterranean environment only recently. This timing difference between sets of pairs can reduce our power to detect a rate variation induced by the shift to a subterranean habitat. For any given species, our substitution rate estimate is an average across the terminal branch of the phylogeny leading to that species, that is, for a period of time that extends to the last observed speciation event. If a species became subterranean recently, relative to this speciation event, and only then evolved a different rate of substitution, its estimated substitution rate on the whole branch will be marginally influenced by this late colonization event. Quantitatively, the magnitude of the observed rate variation will depend directly on the proportion of time along the terminal branch corresponding to underground life (hereafter called the relative colonization time, RCT). This RCT can range from 0 (surface species) to 1 (subterranean species which colonized groundwater when diverging from the paired surface species). If RCT is small, the observed rate variation will be small. We estimated RCT using the pseudogenization of an opsin locus, as described in Lefébure et al. (2017). Concomitantly with the transition to a subterranean habitat, there is a regression of the ocular system that is commonly associated with a loss of function of the opsin genes (Niemiller et al. 2012). We estimated RCT for 23 out of 26 species for which we were able to assemble an opsin gene. Briefly, we assume a two-state model for the opsin gene: a surface and a subterranean state. Before the habitat transition the opsin ratio of nonsynonymous to synonymous substitution rates (d_N/d_S) is very low and mainly influenced by purifying selection. After the habitat transition, the opsin gene evolves under a neutral process with a d_N/d_S ratio equal to one. The estimated opsin d_N/d_S of a subterranean species is therefore a weighted mean of these two d_N/d_S, with weights depending on the ratio between the colonization and the speciation time. From this, we can then estimate the proportion of the RCT and directly test its correlation with d_S.

The estimated values of RCT confirmed that our naive classification into surface and subterranean species hides a more complex scenario. Indeed, some species have colonized the subterranean habitat quickly after speciation whereas others colonized the subterranean habitat much later on (e.g., 2.2% and 76.5% of the terminal branch for *Proasellus jaloniacus* and *Proasellus hercegovinensis*, respectively, fig. 1, supplementary table S1, Supplementary Material online). In the nuclear genome, we recovered a negative correlation between d_S and RCT ($r^2 = 0.43$, table 1, fig. 2). We then tested if a model with the RCT explained a significantly greater part of the d_S variance than a model with only the binary description of the habitat. A model comparison with both explanatory variables to a simpler model with only the binary ecological status favored the former more complex model (LRT P value $= 0.0049$, L ratio $= 7.921$). On the other hand, there was no correlation between the mitochondrial d_S and RCT. The $d_{S_{mito}}/d_{S_{nucl}}$ was significantly correlated to RCT (table 1). On the basis of RCT, species can be empirically split into three groups (see supplementary table S1, Supplementary Material online): 1) the "true surface" species with RCT $<1\%$—these are the six pigmented and occulated species and, surprisingly, the subterranean species Proasellus grafi; 2) the "true subterranean" species for which RCT $> 10\%$—these are the depigmented and anophtalmous species; and 3) the intermediate states ($1\% <$ RCT $< 10\%$) with partially depigmented and microphtalmous species. When only using the habitat status, these intermediate species blur the signal and reduce the estimated correlation because the contrast between the

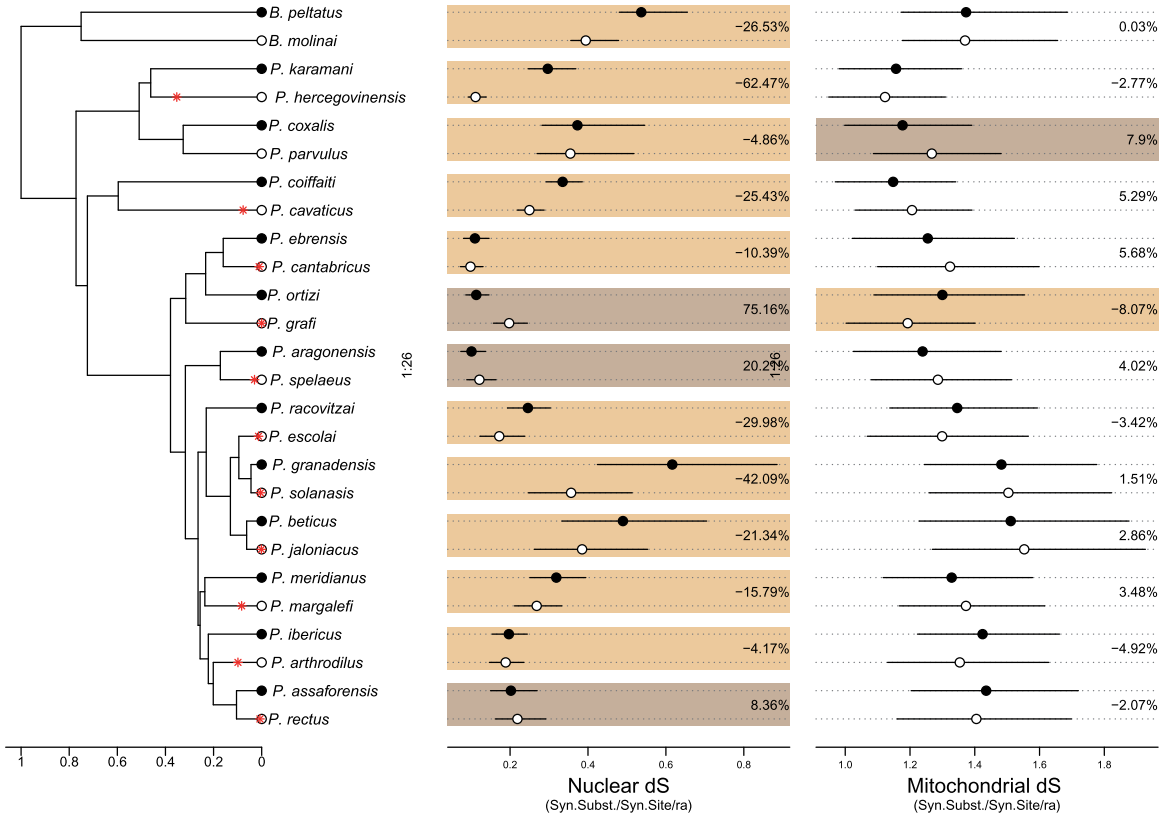

Fig. 1. Substitution rate of the nuclear (center) and mitochondrial (right) genomes in 13 Aselloidea species pairs (left) each composed of one surface species (black circle) and one subterranean species (white circle). The chronogram (left) time scale is arbitrarily defined so that the age of the root is equal to 1. Whenever an opsin gene could be recovered in a subterranean species, a red star on the chronogram indicates the estimated colonization time using opsin gene nonfunctionalization. Rates are synonymous substitutions per synonymous site (d_S) relative to the root age (ra) with their 95% credibility interval as estimated by CoEvol. For each pair, percentage indicates the variation of the substitution rate in the subterranean species relative to the surface species. When this variation has a posterior probability of being different from 0 that is >0.9, the species pair is highlighted with a dark (rate increase) or light (rate decrease) colored box.

Table 1. Phylogenetic Least Square (PGLS) Regression of Nuclear Synonymous Substitution Rate (d_S), Mitochondrial d_S, the d_S Ratio of the Two Compartments and the Number of Mitochondrial Synonymous Transversions (TvS) Against the Ecological Status (surface—subterranean), the Proportion of the Relative Colonization Time (RCT), and the Metabolic Rate (estimated by the RNA/protein ratio).

Dependent Variable	Explanatory Variable	Slope Sign	*L* ratio	*P* value	Pseudo R^2 (Coxsnell)
Nuclear d_S/ra	Ecological status	−	5.516	0.019	0.191
	RCT	−	13.066	3.10−4	0.433
	RNA/protein ratio	+	11.413	7.10−4	0.510
Mitochondrial d_S/ra	Ecological status	+	0.042	0.838	0.002
	RCT	−	0.337	0.562	0.015
	RNA/protein ratio	−	0.771	0.380	0.047
$d_{S_{mito}}/d_{S_{nucl}}$ ratio	Ecological status	+	2.733	0.098	0.100
	RCT	+	8.498	0.004	0.309
	RNA/protein ratio	−	9.258	0.002	0.439
Mitochondrial TvS	Ecological status	+	0.037	0.847	0.001
	RCT	−	0.023	0.881	0.001
	RNA/protein ratio	−	0.342	0.559	0.021

Note.—Each line corresponds to one likelihood ratio test between the models with and without the given explanatory variable.

surface and the subterranean species in these pairs is less strong and is diluted compared with the other pairs. Indeed, the three species pairs that show an inverse variation in the nuclear d_S ($d_{S_{subterranean}} \geq d_{S_{surface}}$) each contain at least one species with this intermediate state (figs. 1 and 2).

RNA/Protein Ratio

Under the hypotheses that the activity of the respiratory chain directly influences the mutation rate, the MR is expected to be positively correlated to the mitochondrial d_S. To test this hypothesis, we used the RNA/protein ratio.

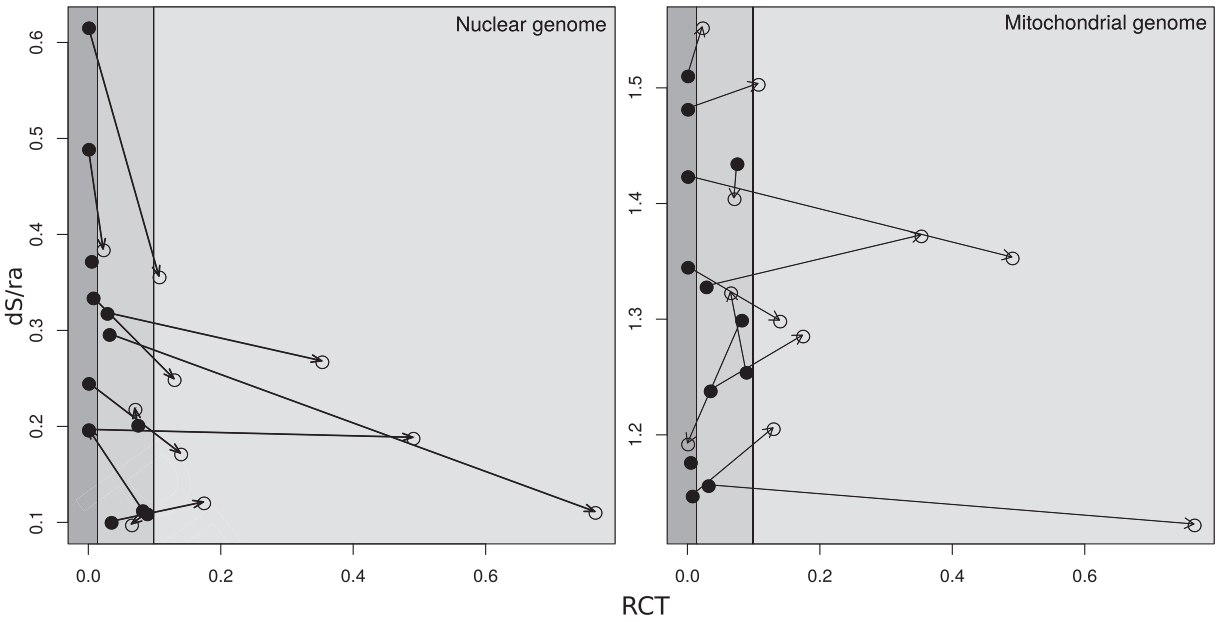

Fig. 2. Relationship between synonymous substitution rate relative to the root age (d_S/ra) and the proportion of the terminal branch that is subterranean (RCT), for the nuclear (left) and mitochondrial (right) genomes. Subterranean species are depicted with white circles and surface species with black circles. The two species of one pair are linked with a black line. Different gray levels indicate species for which the subterranean lifestyle represents <1% of the terminal branch (left) or >10% of the terminal branch (right).

This ratio is a good proxy of the number of active ribosomes per synthesized protein (Cox 2003; Karpinets et al. 2006) and when measured at the organism level it reflects the overall speed at which proteins are renewed. A positive correlation between the RNA/protein and growth rate has been observed in unicellular organisms (Neidhardt and Magasanik 1960; Leick 1968; Cox 2003; Karpinets et al. 2006), in rotifers (Wojewodzic et al. 2011), cephalopods (Houlihan et al. 1990; Pierce et al. 1999), ray-finned fish (Mathers et al. 1992; Peragon et al. 2001), copepoda (Wagner et al. 2001), cladocera (McKEE and Knowles 1987), and even in plants (Xing et al. 2016). Though different from the more commonly used resting oxygen consumption per gram of tissue, this ratio should also be positively correlated with the MR. For example, induced hypermetabolism in mammals is associated with a higher RNA/protein ratio (Tata et al. 1962, 1963). That said, the exact relationship between the RNA/protein ratio, growth rate and MR have yet to be thoroughly tested in Isopods. The RNA/protein ratio was found to be lower in subterranean species (fig. 3, PGLS P-value = 0.03). However, no significant correlation was found between this ratio and the mitochondrial d_S (fig. 3, table 1, PGLS test). On the other hand, the RNA/protein ratio was positively correlated with the nuclear d_S and negatively with the $d_{S_{mito}}/d_{S_{nucl}}$ ratio (PGLS test, table 1).

Confounding Factors and Analytical Bias

Translational Selection

Subterranean species have smaller long-term effective population sizes (Lefébure et al. 2017). While effective population size does not impact the rate of neutral substitution, it can theoretically impact the d_S. Indeed, effective population size affects the efficacy of selection, including translational selection on codon usage, which in turn has an impact on the synonymous rate (Duret and Mouchiroud 1999). For that reason, differences in effective population size might differentially impact the d_S of subterranean and surface species (Chamary et al. 2006). For each data set, we checked for a change in the intensity of translational selection by computing for each codon the difference in the relative synonymous codon usage (ΔRSCU) between the 10% most highly expressed and the 10% most lowly expressed nuclear genes (supplementary table S3, Supplementary Material online). If translational selection is strong, the most highly expressed genes should have a higher frequency of optimal codons (i.e., codons corresponding to the most frequent tRNA). We considered that codons with high and positive ΔRSCU (>0.05) are the optimal codons. Because there are only 13 protein-coding mitochondrial genes, RSCU computation is not reliable for mitochondrial genes. As a substitute, we computed the ENC, the effective number of codons (ENC; Wright 1990). This number varies between 20 (indicating that only a single codon is used for each amino acid) and 61 (indicating that all synonymous codons are used with equal frequency for any one amino-acid). It should be noted that ENC does not directly detect translational selection, however, it is expected to reflect a codon usage bias that can be linked to translational selection. For the nuclear genes, despite a slight trend for an excess of optimal codons in surface than in subterranean species it was not significant (PGLS, P-value = 0.18). Nonetheless this trend cannot explain the observed pattern, as stronger translational selection in surface species should reduce their d_S not increase it. For the mitochondrial genes, ENC ranges between 43 and 55, except for *Bragasellus peltatus* which has an ENC of 38 (supplementary table S1, Supplementary Material online). These values are

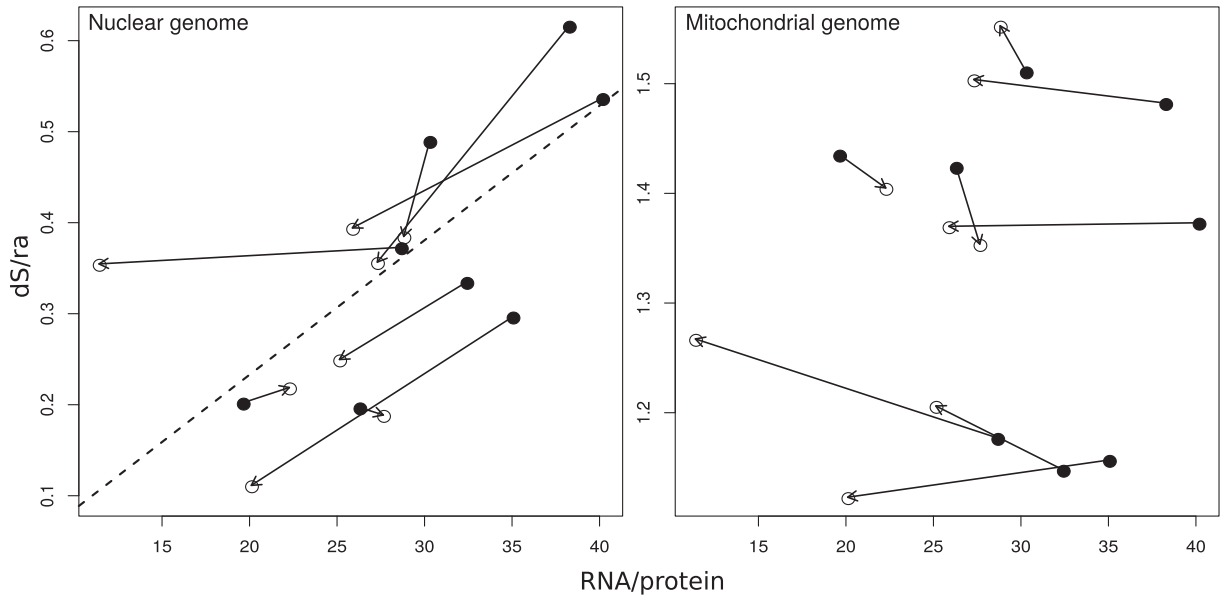

Fig. 3. Relationship between synonymous substitution rate relative to root age (d_S/ra) and the RNA/protein ratio for the nuclear (left) and mitochondrial (right) genomes. Subterranean species are depicted with white circles and surface species with black circles. The two species of one pair are linked with a black line. The dotted line indicates the linear regression estimated using a PGLS.

high (Wright 1990), indicating that there is a weak mitochondrial codon usage bias. Moreover, ENC scores are not correlated with the species habitat (PGLS, P-value = 0.38). Altogether, there is no evidence that selection on synonymous codon usage is biasing the estimated nuclear and mitochondrial d_S.

Ultraviolet (UV) Radiation

The complete absence of UV radiation in subterranean habitats could impact the mutation rate, independently of LHTs variation. UV radiation causes photo-excitation between pyrimidine dimers, which twists the DNA molecule. DNA and RNA polymerases cannot transcribe/copy the damaged bases and instead replace them by two thymine bases (Brash 2015). Thus, any variation in the mutation rate caused by different UV exposures will be accompanied by a concomitant variation in the frequency of the CpT, TpC, CpC, or TpT dinucleotides. To detect a bias in dinucleotide composition, we computed the Z_{score} score statistic proposed by Palmeira et al. (2006). Briefly, this method computes the excess of each dinucleotide in synonymous positions compared with a neutral model based on nucleotide frequencies. We detected no difference in the composition in the four pyrimidine dinucleotides between the surface and subterranean species (fig. 4, Wilcoxon, P-value >0.05), suggesting that the absence of UV in subterranean habitat is not the factor reducing the subterranean nuclear d_S.

Saturation

As mitochondrial genomes evolve faster than nuclear genomes, our estimate of the mitochondrial substitution rate is more prone to be biased by saturation (multiple substitutions at certain nucleotide positions). Stronger saturation in the mitochondrial genome could potentially mask variation in d_S that would otherwise be observable in a non-saturated data-set like the nuclear one. In other words, the observed decoupling between the nuclear and mitochondrial d_S may be the consequence of saturation of the mitochondrial rate. To estimate the level of saturation, we compared the observed divergence (number of differences observed between two sequences) to the patristic divergence along the phylogenetic tree, estimated using a complex model of evolution (GTR + G + I model). The latter estimate of divergence will at least partially compensate for the effect of saturation whereas the former will not (Philippe and Forterre 1999). While mitochondrial third position transitions are quickly saturated, this is not the case for the third position transversions, which vary linearly with the distance between species (supplementary fig. S3, Supplementary Material online). Consequently, to test if saturation hides mitochondrial rate variation, we used the synonymous transversions. As seen with the d_S, the number of mitochondrial synonymous transversions is not correlated with habitat status nor with colonization time (table 1).

Statistical Power

The number of analyzed mitochondrial genes is much lower than the number of nuclear genes (12 vs. 382). The observed lack of mitochondrial rate variation could therefore be the result of a reduced power in the mitochondrial case. By considering only synonymous transversions, this difference in data size is even more pronounced. To test if differences in data size alone might explain the observed differences between the nuclear and mitochondrial genomes, we performed 1,000 resamplings of 26,566 codons in the nuclear alignment to obtain the same number of substitutions in the two compartments (on average 504 synonymous transversions on a terminal branch). We then computed the mean

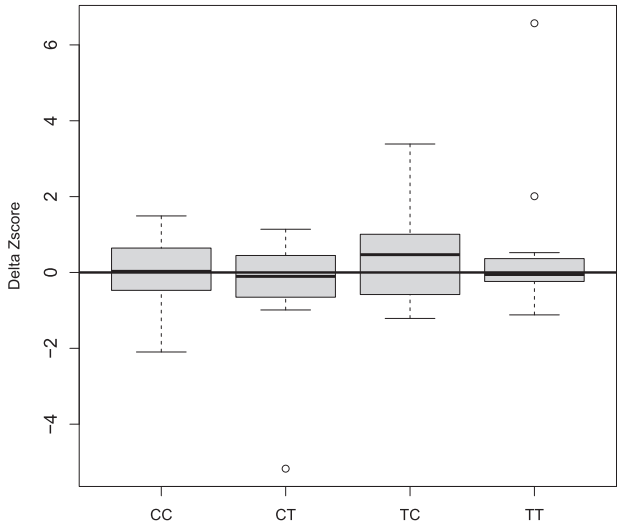

Fig. 4. Delta Z_{score} ($Z_{score_{surface}} - Z_{score_{subterranean}}$) for the four dinucleotide combinations sensitive to UV rays. The Z_{score} (Palmeira et al. 2006) computes the excess of each dinucleotide in synonymous positions compared with a neutral model based on nucleotide frequencies. If the absence of UV exposure in subterranean habitat had a direct influence on the mutation rate, we would observe positive delta Z_{score}.

synonymous transversion contrast $\left[S = \frac{1}{13}\sum_{i=1}^{13}\left(\log\left(\frac{TvS_{surface\,i}}{TvS_{subterranean\,i}}\right)\right)\right]$ for each nuclear sample and for the concatenation of mitochondrial genes, so as to estimate the probability that the mitochondrial genes behave like a subsample of the nuclear genes. This resampling shows that, despite a strong reduction in data size, surface species still display a higher rate of nuclear molecular evolution than subterranean species ($S_{mean} = 0.253$, 95% CI = 0.251–0.254, fig. 5). The mitochondrial contrast is marginally negative and outside the nuclear distribution ($S = -0.04$). Thus, the absence of rate variation in the mitochondrial genome is not linked to a reduced statistical power.

Discussion

Reconsideration of the Main Hypotheses

Subterranean isopod species evolved a lower nuclear substitution rate but kept a steady mitochondrial rate. This observation does not correspond to any of the predictions borne out of the two main bodies of hypotheses proposed in the literature, namely those linked to the rate of duplication and those linked to the activity of the respiratory chain, at least in their commonly accepted forms. The two hypotheses linked to the activity of the respiratory chain are based on the idea that the ROS production influences the rate of mutation. Because ROS are produced in the mitochondria, these two hypotheses would both imply a more pronounced decrease in d_S in the mitochondrial genome than in the nuclear genome. Under the rate of duplication hypothesis one would expect a decrease in d_S in subterranean species relative to surface species of the same magnitude in the two genomic compartments. We saw no correlation between the RNA/protein ratio—a proxy for MR—and the mitochondrial d_S. These results are robust to the effect of different colonization timings, to potential confounding factors (differences in codon usage bias and UV exposure) and to methodological bias (differences in the level of saturation and data size). Surprisingly, whereas the RNA/protein ratio is not correlated with the mitochondrial d_S, it is strongly correlated with the nuclear d_S. Although this method needs further testing to be apply to these isopods, absence of correlation for the mitochondrial d_S is in accordance with previous studies, which found no correlation between MR and mitochondrial substitution rate (Lanfear et al. 2007). A direct impact of the MR on the nuclear genome but not on the mitochondrial one is highly unlikely because the mutagenic agents, here the ROS, are produced in the mitochondria and should impact it first. As the MR is often strongly correlated to GT (Martin and Palumbi 1993), the correlation between RNA/protein ratio and the nuclear d_S suggests that the GT—rather than the MR—does indeed impact the rate of substitution but that it does so only in the nuclear genome. In addition, it supports the view that the activity of the respiratory chain, either directly through the production of ROS and indirectly through longevity, has little to no impact on either the mitochondrial or the nuclear substitution rates. These results are in accordance with a previous study which showed that mutations due to ROS are negligible compared with other sources of mutation such as errors of the γ polymerase (Larsson 2010).

Decoupling of the Two Genomes by Independent Replication Cycles

Contrary to the predictions raised by earlier hypotheses, mitochondrial d_S does not appear to be impacted by the same factors that impact nuclear d_S. We found that the $d_{S_{mito}}/d_{S_{nucl}}$ ratio varies extensively across species, showing an increase in subterranean species. This result is not a byproduct of saturation, a lack of statistical power, or other confounding factors (UV and translational selection). Allio et al. (2017) also reported extensive ratio of mitochondrial to nuclear mutation rate variation among animal phyla, with a major shift between nonvertebrates and vertebrates (~6 vs. ~20, respectively). However, our results point to a variation in $d_{S_{mito}}/d_{S_{nucl}}$ over a much smaller phylogenetic scale. We observed substantial variation across species (3.3–40.3) of the same magnitude as that reported by Allio et al. (2017) across phyla (supplementary table S2, Supplementary Material online). Instead of different $d_{S_{mito}}/d_{S_{nucl}}$ per phyla, we propose that there is a complete and permanent decoupling of the mitochondrial and nuclear rates across all taxa. In our data set, but also in Allio et al.'s data, the mitochondrial rate varied very little. Therefore, decoupling in these two data sets is apparently controlled by variation in the nuclear rate alone, which we suggest is driven by a GT effect.

To accommodate this observation, we propose a model in which the nuclear and mitochondrial d_S are decoupled, fundamentally because these two genomes have independent replication cycles. Available data in Asellidae (Henry 1976) indicate a general lengthening of all stages across the life cycle (lengthening of the embryonic stages, puberty postponement, and increased lifespan) in subterranean species. On the basis of the principle that most mutations occur during

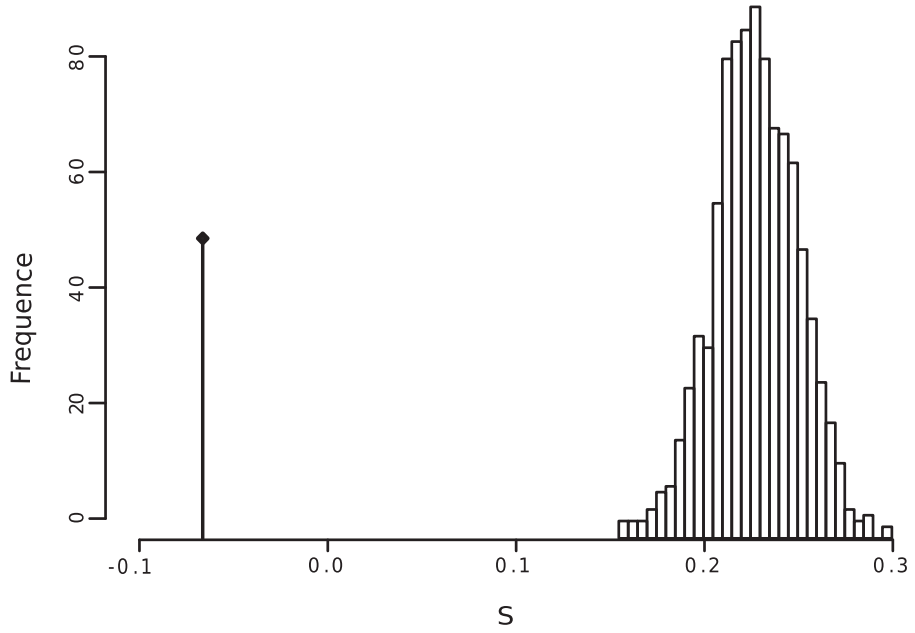

Fig. 5. Testing if the observed uncoupling between the nuclear and mitochondrial rates is due to a data-set size difference by subsampling the nuclear data-set. The statistic $\left[S = \frac{1}{13}\sum_{i=1}^{13}\left(\log\left(\frac{TvS_{surface_i}}{TvS_{subterranean_i}}\right)\right)\right]$ was computed on 1,000 resampling of 26,566 codons of the nuclear alignment (in white) and on the mitochondrial alignment (black line). $TvS_{surface_i}$ is the number of synonymous transversions estimated on the terminal branch leading to the surface species in the pair *i* and $TvS_{subterranean_i}$ is the analogous estimates in the subterranean species of the pair.

genome replication (Gangloff et al. 2017), we can then assume that a lengthening of the GT leads to a decrease in the cell duplication rate, inducing a decrease in the nuclear substitution rate. If the mitochondrial replication rate does not change accordingly, then this could explain why GT as not effect on the mitochondrial substitution rate. We propose that the number of nuclear genome replication per unit of time reduces in the subterranean species as a by-product of a longer GT, but that the number of mitochondrial genome replication per unit of time is stable. In other words, the rate of mitochondrial replication does not seem to be correlated to the rate of germ stem cell mitosis in these species.

Gametogenesis May Control Rate Decoupling

The differential impact of LHT on the two metazoan genomic compartments was unexpected and, to the best of our knowledge, has not been explicitly described in previous studies. Thus far, most studies have tested only small numbers of nuclear genes and were almost exclusively devoted to the study of mammals or birds. These two endothermic taxa present particularities in their gametogenesis. In these organisms, primary oocytes are formed during embryonic development where they begin meiosis and are stopped in prophase I. Then, oocytes stay in a quiescent state until just before ovulation. Over this time, mitochondria replicate very little or not at all (de Paula et al. 2013), imposing a synchronization of replication of the mitochondrial and nuclear genomes. If the rate of mutation is mainly governed by the rate of genome replication, and even if the nuclear and mitochondrial replication rates are independent, the observed coupling between the two rates in mammals and birds could be a result of this imposed gametic synchronization. In contrast, in arthropods, gametogenesis is continuous: primitive germ cells (germ stem cells) undergo mitosis during the entire life of the organism, and a small fraction of these stem cells periodically commence meiosis (Charniaux-Cotton 1973). As such, gametogenesis does not impose replication synchronization, allowing a complete uncoupling of the mitochondrial and nuclear mutation rates in arthropods. It should be noted that spermatogenesis in mammals is similar to arthropod gametogenesis. However, as mitochondria transmission is strictly maternal, this should not influence the mitochondrial mutation rate.

Aging and Mutation Rate

The absence of any influence of the activity of the respiratory chain, whether direct (MR hypothesis) or indirect (longevity hypothesis), on the mitochondrial d_S suggests that mitochondrial metabolism has little influence on the germline mutation rate. These results are in accordance with the point of view that the mitochondrial theory of aging implies an oversimplistic link between MR, ROS production and mutation (Lapointe and Hekimi 2010). Indeed, the absence of an influence of the activity of the respiratory chain on the germline mutation rate can be explained by two nonexclusive hypotheses. First, an increased longevity is not necessarily accompanied by better ROS management. Indeed, Jobson et al. (2010) showed no consistent variation in d_N/d_S in genes linked to oxidative stress in long-lived mammals. On the other hand, they found a lower d_N/d_S in genes coding for lipid composition of cellular membrane. Membrane fatty acid composition modulates the resistance to oxidative damage. Thus, a strategy to increase possible lifespan may not be to reduce ROS production and damage, but instead, to improve tissue resistance. This strategy would have no impact on the rate of

molecular evolution and may explain the absence of a correlation between the RNA/protein ratio and the mitochondrial d_S. This is particularly likely as the impact of ROS on the mitochondrial mutation rate seems to be marginal (Larsson 2010). Second, a differential impact of ROS in somatic cells between long- and short-lived species does not necessarily mean that this difference exists in germinal cells. The longevity hypothesis is based on the mitochondrial theory of aging. This theory proposes that ROS produced by metabolic activity over the life of an organism would cause mutations in the mitochondrial genome, which would then lead to a senescent phenotype. The longevity hypothesis makes the assumption that these mechanisms are ubiquitous, namely that the selective pressure to decrease the somatic mutation rate leads to an overall decrease in the germinal mutation rate. However, the activity of the respiratory chain is lower in germinal cells than in somatic cells (de Paula et al. 2013), and thus germinal cells have less ROS exposure. It is therefore possible that the mechanism in place in somatic cells to reduce the impact of ROS is not active in the germline. Thus, the somatic mutation rate can be decoupled from the germinal mutation rate and respond differently to LHT variation. Altogether, we propose that ROS have only a limited influence on the substitution rate.

Conclusion

We have showed that in isopods, increased GT in subterranean species is correlated with decreased nuclear substitution rate but that neither the activity of the respiratory chain nor the GT or longevity influenced the mitochondrial substitution rate. We propose that this complete decoupling between the nuclear and mitochondrial rate is linked to the fact that these two compartments are not subjected to the same replication schedule during development. Most prior studies have been based on few genes, rarely nuclear, and have been biased toward mammals and birds which have peculiar gametogenesis and metabolism. The hypotheses that were developed from these studies (namely the GT, MR, and longevity hypotheses) fit poorly with our observations, which puts their universality into question. We suggest that the rate of substitution is mainly controlled by the number of duplications until fertilization per unit of time which will depend on the type of gametogenesis, the organelle and the GT.

Materials and Methods

Data Acquisition

Nuclear Genes

Three hundred and eighty six one-to-one orthologous nuclear genes from 13 species pairs (sensu Felsenstein 2004) were retrieved from a study by Francois et al. (2016) (http://dx.doi.org/10.5281/zenodo.53830; last accessed October 06, 2018). This data set was built using de novo assembled transcriptomes (ENA project PRJEB14193) followed by gene family definition and ortholog sequence extraction using a tree pattern (Dufayard et al. 2005). Four genes presenting suspicious gene tree topologies or branch lengths were filtered out to avoid potential contaminants (FAM000151_1, FAM000919_1, FAM000990_2, FAM003078_1).

Mitochondrial Genes

Mitochondrial genes were not present amongst the 382 genes obtained above. Indeed, owing to a different genetic code in invertebrate mitochondria, mitochondrial ORFs were systematically missed by the ORF caller (Transdecoder) used by Francois et al. (2016). We reconstructed mitochondrial genomes using both the de novo transcriptome assemblies from Francois et al. (2016) and low coverage genome sequencing reads available for 22 species from Lefébure et al. (2017). Since mitochondrial genomes are present in multiple copies per cell, a very low sequencing effort is sufficient to yield a high coverage for mitochondrial sequences. Using the DNA-seq reads, mitogenomes were assembled with MITObim (Hahn et al. 2013) using the COI gene as a seed to build the complete mitogenome. For the four species without DNA-seq reads (*P. ebrensis*, *P. cantabricus*, *P. ortizi*, and *P. graffi*), large mitochondrial contigs were built with MITObim by using RNA-seq reads and the mitochondrial genes from the closest possible species (taken from the previous 22 species with assembled mitogenomes) as seeds. The mitochondrial genome from this closest species was used as a reference to map the RNA contigs and to assemble complete mitogenomes. Mitochondrial genomes were annotated using the MITOS web server (Bernt et al. 2013, supplementary fig. S2, Supplementary Material online). We recovered 12 mitochondrial protein-coding genes (*cytb*, *cox1*, *cox2*, *cox3*, *atp6*, *nad1*, *nad2*, *nad3*, *nad4*, *nad4l*, *nad5*, *nad6*) for each of the 26 species. Because of its short size, *atp8* was difficult to identify and delimit, and was thus not included in subsequent analyses. Mitochondrial genes were aligned with PRANK (Löytynoja and Goldman 2008) and sites ambiguously aligned were removed with Gblocks (Castresana 2000). The 382 nuclear and 12 mitochondrial gene alignments used in this study have been deposited on Zenodo (https://doi.org/10.5281/zenodo.1409532; last accessed October 06, 2018).

Rate of Molecular Evolution

We used the synonymous substitution rate (d_S) as a proxy for the mutation rate. Genes were concatenated independently for the nuclear and the mitochondrial compartment. Phylogenetic tree was built with the 382 nuclear genes with PhyML v3.0 (Guindon et al. 2010) under a GTR + G + I model with 500 bootstrap replicates and was rooted using the *Bragasellus* lineage as an outgroup. Synonymous substitution rates per unit of time were estimated using CoEvol (Lartillot and Poujol 2012). This software program implements a Muse and Gaut codon model (Muse and Gaut 1994), with Brownian variation in d_S and omega $= d_N/d_S$ along the tree. Bayesian inference and reconstruction of the history of variation in d_S and d_N/d_S along the tree is conducted by Markov Chain Monte Carlo (MCMC). Two independent chains were run, and were stopped after checking for convergence by eye and with the tracecomp program included in the Coevol package (effective sample size > 300

and discrepancy between chains < 0.1 for all statistics). Chains were stopped after 29,713 generations (burn-in excluded) for mitochondrial genomes, and 4,001 generations (burn-in excluded) for nuclear genomes. The age of the root was arbitrarily set to 1, resulting in synonymous substitution rate estimates that are relative to the root age (d_S/ra). The 26 assembled mitogenomes were deposited to the ENA under the accession number from ERZ724045 to ERZ724070.

Colonization Time

The relative colonization time (RCT), which is the proportion of the branch corresponding to a subterranean lifestyle was estimated using the nonfunctionalization of the opsin I gene locus as in Lefébure et al. (2017). Assuming a two-state model of evolution with one surface opsin d_N/d_S estimated using opsins from surface species, and one subterranean opsin d_N/d_S equal to 1, we estimated the colonization time (t) as a function of the speciation time (T) and the estimated opsin d_N/d_S measured on a given branch leading to a subterranean species (supplementary table S1, Supplementary Material online):

$$\mathrm{RCT} = \frac{t}{T} = \frac{d_N/d_{S_{subterranean}} - d_N/d_{S_{surface}}}{1 - d_N/d_{S_{surface}}}$$

d_N/d_S was estimated using the CodeML program in the PAML package (Yang 2007). $d_N/d_{S_{surface}}$ was computed using the mean of opsin d_N/d_S of the six oculated and pigmented species (*P. ibericus*, *P. beticus*, *P. meridianus*, *P. coxalis*, *P. coiffaiti*, and *P. karamani*). We retrieved opsin sequences for 19 species from Lefébure et al. (2017) and complemented this data set with four additional species (*P. ebrensis*, *P. cantabricus*, *P. ortizi*, and *P. graffi*), using a combination of Sanger sequencing, transcriptome assemblies and genome sequencing reads. In accordance with Lefébure et al. (2017), this opsin locus was not found in the two species of the genus *Bragasellus* and in one *Proasellus* subterranean species (*P. parvulus*). The opsin alignment used in this study has been deposited on Zenodo (https://doi.org/10.5281/zenodo.1409532).

RNA/Protein Ratio

As in Lefébure et al. (2017), we used the RNA/protein ratio as a proxy for MR. For 16 species, we recovered the RNA/protein ratio from Lefébure et al. (2017). Briefly, for 10 individuals per species, total RNA and proteins were extracted with a TRI-Reagent protocol (Molecular Research Center). Total RNA was quantified by fluorimetry (Qubit; Life technologies) and total protein were obtained using the Bicinchoninic acid assay (Smith et al. 1985). The RNA/protein ratio was then estimated by the total RNA normalized by the total protein biomass (supplementary table S1, Supplementary Material online).

Confounding Factors and Analytical Bias

Synonymous Codon Usage

The RSCU corresponds to the number of times a given codon is observed, relative to the number of times this codon would be observed under a uniform synonymous codon usage (i.e., with all the codons for a given amino-acid having the same probability). Optimal codons are defined by a higher RSCU value in highly expressed transcripts (Duret and Mouchiroud 1999). Thus, optimal codons were identified by subtracting, for each codon, the RSCU averaged over the 10% transcripts having the lowest expression level to the RSCU averaged over the 10% most highly expressed transcripts. Expression of each contig was estimated with RSEM (Li and Dewey 2011). The 10% most highly expressed and the 10% most lowly expressed contigs were selected based on TPM (transcript per million) estimates (Li et al. 2010; Wagner et al. 2012). RSCU indices were calculated using the seqinR R package (Charif and Lobry 2007). The ENC was computed for each species on the concatenation of the 12 mitochondrial genes with the vhica R package (Wallau et al. 2016).

UV Radiation

To test if UV radiation affects the rate of molecular evolution of surface species, we estimated dinucleotide frequencies using the Z_{score} statistic proposed by Palmeira et al. (2006) in the seqinR package (Charif and Lobry 2007). We computed this statistic on the concatenation of the 382 nuclear genes under a "syncodon" model with 1,000 permutations (supplementary table S4, Supplementary Material online). This method considers the nucleotide frequency and the codon structure. Because changes in the second position of the codon are never synonymous, only changes in dinucleotides in the first and the third position of the codon are taken into account. Thus, this method produces results similar to what would be measured in neutrally evolving regions.

Saturation and Power

To reduce the influence of saturation on d_S estimates, we computed synonymous transversions with the Bio++ suite (Dutheil and Boussau 2008). A nonhomogenous model (NY68 model) model was first applied to the mitochondrial alignment with BppML and then the MapNH program (Version 1.1.1) of the TestNH package (Guéguen and Duret 2018) was used to reconstruct the ancestral states and to estimate the number of synonymous transversions on each branch (supplementary table S5, Supplementary Material online). The relation between synonymous transversion number and ecology, colonization time and RNA/protein ratio was tested with a PGLS.

Comparative Analyses

Correlations between the rate of molecular evolution and habitat, RCT and RNA/protein ratio were tested by a Phylogenetic Generalised Least Squares (PGLS, Martins and Hansen 1997). Tests were performed by using the nlme (Pinheiro et al. 2014) and ape packages (Paradis et al. 2004) in R (R Core Team 2014). The output chronogram built by CoEvol on the 382 nuclear genes was used to correct for phylogenetic inertia. Second, for each pair composed of a surface and a subterranean species, and based on the output of Coevol, we computed the posterior probability of an

increase of the d_S in surface species as the percentage of point of the Monte-Carlo chain where the surface species has a higher d_S than the subterranean species.

Supplementary Material

Supplementary data are available at *Molecular Biology and Evolution* online.

Acknowledgments

This work was supported by the Agence Nationale de la Recherche (ANR-15-CE32-0005 Convergenomix, France) and the CNRS (APEGE No. 70632, PEPS ExoMod 2014 and Enviromics 2014, France). We gratefully acknowledge support from the CNRS/IN2P3 Computing Center (Lyon/Villeurbanne—France), for providing a significant amount of the computing resources needed for this work. We thank Florian Mermillot-Blondin and Laurent Simon for their help in the field and for the RNA/protein ratio measurement. We are grateful to Benoît Nabholz, Nicolas Galtier, Marie Semon, and Carine Rey for helpful discussions. We also thank Laura Grice for her comments and suggestions in the latter stages of manuscript preparation, as well as two anonymous reviewers for their helpful comments.

References

Allio R, Donega S, Galtier N, Nabholz B. 2017. Large variation in the ratio of mitochondrial to nuclear mutation rate across animals: implications for genetic diversity and the use of mitochondrial DNA as a molecular marker. *Mol Biol Evol*. 34(11):2762–2772.

Baer CF, Miyamoto MM, Denver DR. 2007. Mutation rate variation in multicellular eukaryotes: causes and consequences. *Nat Rev Genet*. 8(8):619–631.

Barja G. 2007. Mitochondrial oxygen consumption and reactive oxygen species production are independently modulated: implications for aging studies, *Rejuvenation research*, 10(2):215–224.

Barja G. 2002. Endogenous oxidative stress: relationship to aging, longevity and caloric restriction. *Ageing Res Rev*. 1(3):397–411.

Bernt M, Donath A, Jühling F, Externbrink F, Florentz C, Fritzsch G, Pütz J, Middendorf M, Stadler PF. 2013. MITOS: improved de novo metazoan mitochondrial genome annotation. *Mol Phylogenet Evol*. 69(2):313–319.

Brash DE. 2015. UV signature mutations. *Photochem Photobiol*. 91(1):15–26.

Bromham L, Hua X, Lanfear R, Cowman PF. 2015. Exploring the relationships between mutation rates, life history, genome size, environment, and species richness in flowering plants. *Am Nat*. 185(4):507–524.

Bromham L, Rambaut A, Harvey PH. 1996. Determinants of rate variation in mammalian DNA sequence evolution. *J Mol Evol*. 43(6):610–621.

Caccone A, Gentile G, Burns CE, Sezzi E, Bergman W, Ruelle M, Saltonstall K, Powell JR. 2004. Extreme difference in rate of mitochondrial and nuclear DNA evolution in a large ectotherm, Galápagos tortoises. *Mol Phylogenet Evol*. 31(2):794–798.

Castresana J. 2000. Selection of conserved blocks from multiple alignments for their use in phylogenetic analysis. *Mol Biol Evol*. 17(4):540–552.

Chamary JV, Parmley JL, Hurst LD. 2006. Hearing silence: non-neutral evolution at synonymous sites in mammals. *Nat Rev Genet*. 7(2):98.

Charif D, Lobry JR. 2007. SeqinR 1.0-2: a contributed package to the R project for statistical computing devoted to biological sequences retrieval and analysis. In: Bastolla U, Porto M, Roman HE, Vendruscolo M, editors. Structural Approaches to Sequence Evolution. Berlin, Heidelberg: Springer Berlin Heidelberg, 207–232.

Charniaux-Cotton. 1973. Description et contrôle de l'ovogenèse chez les Crustacés supérieurs. *Ann Biol Anim Biochim Biophys*. 13:21–37.

Cox RA. 2003. Correlation of the rate of protein synthesis and the third power of the RNA: protein ratio in *Escherichia coli* and *Mycobacterium tuberculosis*. *Microbiology* 149(Pt 3):729–737.

Doublet V, Raimond R, Grandjean F, Lafitte A, Souty-Grosset C, Marcadé I. 2012. Widespread atypical mitochondrial DNA structure in isopods (Crustacea, Peracarida) related to a constitutive heteroplasmy in terrestrial species. *Genome* 55(3):234–244.

Dufayard JF, Duret L, Penel S, Gouy M, Rechenmann F, Perrière G. 2005. Tree pattern matching in phylogenetic trees: automatic search for orthologs or paralogs in homologous gene sequence databases. *Bioinformatics* 21(11):2596–2603.

Duret L, Mouchiroud D. 1999. Expression pattern and, surprisingly, gene length shape codon usage in Caenorhabditis, Drosophila, and Arabidopsis. *Proc Natl Acad Sci U S A*. 96(8):4482–4487.

Duret L, Mouchiroud D. 2000. Determinants of substitution rates in mammalian genes: expression pattern affects selection intensity but not mutation rate. *Mol Biol Evol*. 17(1):68–070.

Dutheil J, Boussau B. 2008. Non-homogeneous models of sequence evolution in the Bio++ suite of libraries and programs. *BMC Evol Biol*. 8:1.

Ellegren H, Smith NG, Webster MT. 2003. Mutation rate variation in the mammalian genome. *Curr Opin Genet Dev*. 13(6):562–568.

Felsenstein J. 2004. Inferring phylogenies, volume 2. Sunderland (MA): Sinauer Associates.

Francois CM, Mermillod-Blondin F, Malard F, Fourel F, Lécuyer C, Douady CJ, Simon L. 2016. Trophic ecology of groundwater species reveals specialization in a low-productivity environment. *Funct Ecol*. 30(2):262–273.

Galtier N, Jobson RW, et al. 2009. Mitochondrial whims: metabolic rate, longevity and the rate of molecular evolution. *Biol Lett* 5(3):413–6.

Galtier N, Nabholz B, et al. 2009. Mitochondrial DNA as a marker of molecular diversity: a reappraisal. *Mol Ecol*. 18(22):4541–4550.

Gangloff S, Achaz G, Francesconi S, Villain A, Miled S, Denis C, Arcangioli B. 2017. Quiescence unveils a novel mutational force in fission yeast. *eLife* 6:e27469.

Gillooly JF, Allen AP, West GB, Brown JH. 2005. The rate of DNA evolution: effects of body size and temperature on the molecular clock. *Proc Natl Acad Sci U S A*. 102(1):140–145.

Guéguen L, Duret L. 2018. Unbiased estimate of synonymous and nonsynonymous substitution rates with nonstationary base composition. *Mol Biol Evol*. 35(3):734–742.

Guindon S, Dufayard JF, Lefort V, Anisimova M, Hordijk W, Gascuel O. 2010. New algorithms and methods to estimate maximum-likelihood phylogenies: assessing the performance of PhyML 3.0. *Syst Biol*. 59(3):307–321.

Hahn C, Bachmann L, Chevreux B. 2013. Reconstructing mitochondrial genomes directly from genomic next-generation sequencing reads—a baiting and iterative mapping approach. *Nucleic Acids Res*. 41(13):e129.

Henry JPA. 1976. Recherches sur les Asellidae hypogés de la lignée cavaticus: Crustacea, Isopoda, Asellota. [s.n.]. [S.l.].

Houlihan DF, McMillan DN, Agnisola C, Genoino IT, Foti L. 1990. Protein synthesis and growth in *Octopus vulgaris*. *Mar Biol*. 106(2):251–259.

Hüppop K. 1987. Food-finding ability in cave fish (*Astyanax fasciatus*). *Int J Speleol*. 16(1):4.

Jeschke JM, Kokko H. 2009. The roles of body size and phylogeny in fast and slow life histories. *Evol Ecol*. 23(6):867–878.

Jobson RW, Nabholz B, Galtier N. 2010. An evolutionary genome scan for longevity-related natural selection in mammals. *Mol Biol Evol*. 27(4):840–847.

Karpinets TV, Greenwood DJ, Sams CE, Ammons JT. 2006. RNA: protein ratio of the unicellular organism as a characteristic of phosphorous and nitrogen stoichiometry and of the cellular requirement of ribosomes for protein synthesis. *BMC Biol*. 4:30.

Kennedy SR, Salk JJ, Schmitt MW, Loeb LA. 2013. Ultra-sensitive sequencing reveals an age-related increase in somatic mitochondrial

mutations that are inconsistent with oxidative damage. *PLOS Genet*. 9(9):e1003794.
Kilpert F, Held C, Podsiadlowski L. 2012. Multiple rearrangements in mitochondrial genomes of Isopoda and phylogenetic implications. *Mol Phylogenet Evol*. 64(1):106–117.
Kilpert F, Podsiadlowski L. 2006. The complete mitochondrial genome of the common sea slater, *Ligia oceanica* (Crustacea, Isopoda) bears a novel gene order and unusual control region features. *BMC Genomics*. 7:241.
Kujoth GC, Bradshaw PC, Haroon S, Prolla TA. 2007. The role of mitochondrial DNA mutations in mammalian aging. *PLoS Genetics*. 4:161–173.
Lanfear R, Thomas JA, Welch JJ, Brey T, Bromham L. 2007. Metabolic rate does not calibrate the molecular clock. *Proc Natl Acad Sci U S A*. 104(39):15388–15393.
Lapointe J, Hekimi S. 2010. When a theory of aging ages badly. *Cell Mol Life Sci*. 67(1):1–8.
Larsson NG. 2010. Somatic mitochondrial DNA mutations in mammalian aging. *Annu Rev Biochem*. 79:683–706.
Lartillot N, Delsuc F. 2012. Joint reconstruction of divergence times and life-history evolution in placental mammals using a phylogenetic covariance model. *Evolution* 66(6):1773–1787.
Lartillot N, Poujol R. 2011. A phylogenetic model for investigating correlated evolution of substitution rates and continuous phenotypic characters. *Mol Biol Evol*. 28(1):729–744.
Lefébure T, Morvan C, Malard F, et al. (17 co-authors). 2017. Less effective selection leads to larger genomes. *Genome Res*. 27:1016–1028.
Leick V. 1968. Ratios between contents of DNA, RNA and protein in different micro-organisms as a function of maximal growth rate. *Nature* 217(5134):1153–1155.
Li B, Dewey CN. 2011. RSEM: accurate transcript quantification from RNA-Seq data with or without a reference genome. *BMC Bioinformatics*. 12:1.
Li B, Ruotti V, Stewart RM, Thomson JA, Dewey CN. 2010. RNA-Seq gene expression estimation with read mapping uncertainty. *Bioinformatics* 26(4):493–500.
Li WH, Tanimura M, Sharp PM. 1987. An evaluation of the molecular clock hypothesis using mammalian DNA sequences. *J Mol Evol*. 25(4):330–342.
Lynch M. 2010. Evolution of the mutation rate. *Trends Genet*. 26(8):345–352.
Löytynoja A, Goldman N. 2008. Phylogeny-aware gap placement prevents errors in sequence alignment and evolutionary analysis. *Science* 320(5883):1632–1635.
Martin AP, Naylor GJP, Palumbi SR. 1992. Rates of mitochondrial DNA evolution in sharks are slow compared with mammals. *Nature* 357(6374):153.
Martin AP, Palumbi SR. 1993. Body size, metabolic rate, generation time, and the molecular clock. *Proc Natl Acad Sci U S A*. 90(9):4087–4091.
Martins EP, Hansen TF. 1997. Phylogenies and the comparative method: a general approach to incorporating phylogenetic information into the analysis of interspecific data. *Am Nat*. 149(4):646–667.
Mathers EM, Houlihan DF, Cunningham MJ. 1992. Nucleic acid concentrations and enzyme activities as correlates of growth rate of the saithe *Pollachius virens*: growth-rate estimates of open-sea fish. *Mar Biol*. 112(3):363–369.
McKEE MJ, Knowles CO. 1987. Levels of protein, RNA, DNA, glycogen and lipid during growth and development of Daphnia magna Straus (Crustacea: cladocera). *Freshw Biol*. 18(2):341–351.
Mooers AO, Harvey PH. 1994. Metabolic rate, generation time, and the rate of molecular evolution in birds. *Mol Phylogenet Evol*. 3(4):344–350.
Morvan C, Malard F, Paradis E, Lefébure T, Konecny-Dupré L, Douady CJ. 2013. Timetree of aselloidea reveals species diversification dynamics in groundwater. *Syst Biol*. 62(4):512–522.
Muse SV, Gaut BS. 1994. A likelihood approach for comparing synonymous and nonsynonymous nucleotide substitution rates, with application to the chloroplast genome. *Mol Biol Evol*. 11(5):715–724.
Nabholz B, Glémin S, Galtier N. 2008. Strong variations of mitochondrial mutation rate across mammals—the longevity hypothesis. *Mol Biol Evol*. 25(1):120–130.
Neidhardt FC, Magasanik B. 1960. Studies on the role of ribonucleic acid in the growth of bacteria. *Biochim Biophys Acta*. 42:99–116.
Niemiller ML, Near TJ, Fitzpatrick BM. 2012. Delimiting species using multilocus data: diagnosing cryptic diversity in the Southern Cavefish, Typhlichthys Subterraneus (teleostei: Amblyopsidae). *Evolution* 66(3):846–866.
Nikolaev SI, Montoya-Burgos JI, Popadin K, Parand L, Margulies EH, et al. 2007. Life-history traits drive the evolutionary rates of mammalian coding and noncoding genomic elements. *Proc Natl Acad Sci U S A*. 104(51):20443–20448.
Ohta T. 1993. An examination of the generation-time effect on molecular evolution. *Proc Natl Acad Sci U S A*. 90(22):10676–10680.
Palmeira L, Guéguen L, Lobry JR. 2006. UV-targeted dinucleotides are not depleted in light-exposed prokaryotic genomes. *Mol Biol Evol*. 23(11):2214–2219.
Paradis E, Claude J, Strimmer K. 2004. APE: analyses of phylogenetics and evolution in R language. *Bioinformatics* 20(2):289–290.
de Paula WBM, Lucas CH, Agip A-NA, Vizcay-Barrena G, Allen JF. 2013. Energy, ageing, fidelity and sex: oocyte mitochondrial DNA as a protected genetic template. *Philos Trans R Soc B*. 368(1622):20120263.
Peragon J, Barroso JB, Garcia-Salguero L, de la Higuera M, Lupianez JA. 2001. Growth, protein-turnover rates and nucleic-acid concentrations in the white muscle of rainbow trout during development. *Int J Biochem Cell Biol*. 33(12):1227–1238.
Philippe H, Forterre P. 1999. The rooting of the universal tree of life is not reliable. *J Mol Evol*. 49(4):509–523.
Pierce GJ, Key LN, Boyle PR, Siegert KJ, Gonçalves JM, Porteiro FM, Martins HR. 1999. RNA concentration and the RNA to protein ratio in cephalopod tissues: sources of variation and relationship with growth rate. *J Exp Mar Biol Ecol*. 237(2):185–201.
Pinheiro J, Bates D, DebRoy S, Sarkar D, R Core Team. 2014. nlme: linear and nonlinear mixed effects models. R package version 3.1-117.
R Core Team. 2014. R: a language and environment for statistical computing. Vienna, Austria: R Foundation for Statistical Computing.
Raimond R, Marcadé I, Bouchon D, Rigaud T, Bossy JP, Souty-Grosset C. 1999. Organization of the large mitochondrial genome in the isopod *Armadillidium vulgare*. *Genetics* 151(1):203–210.
Renault D, Hervant F, Vernon P. 2002. Comparative study of the metabolic responses during food shortage and subsequent recovery at different temperatures in the adult lesser mealworm, Alphitobius diaperinus (Coleoptera: tenebrionidae). *Physiol Entomol*. 27(4):291–301.
Richter C, Park JW, Ames BN. 1988. Normal oxidative damage to mitochondrial and nuclear DNA is extensive. *Proc Natl Acad Sci U S A*. 85(17):6465–6467.
Smith PK, Krohn RI, Hermanson GT, Mallia AK, Gartner FH, Provenzano MD, Fujimoto EK, Goeke NM, Olson BJ, Klenk DC. 1985. Measurement of protein using bicinchoninic acid. *Anal Biochem*. 150(1):76–85.
Smith SA, Donoghue MJ. 2008. Rates of molecular evolution are linked to life history in flowering plants. *Science* 322(5898):86–89.
Tata JR, Ernster L, Lindberg O. 1962. Control of basal metabolic rate by thyroid hormones and cellular function. *Nature* 193:1058–1060.
Tata JR, Ernster L, Lindberg O, Arrhenius E, Pedersen S, Hedman R. 1963. The action of thyroid hormones at the cell level. *Biochem J*. 86:408–428.
Thomas JA, Welch JJ, Lanfear R, Bromham L. 2010. A generation time effect on the rate of molecular evolution in invertebrates. *Mol Biol Evol*. 27(5):1173–1180.
Wagner GP, Kin K, Lynch VJ. 2012. Measurement of mRNA abundance using RNA-seq data: RPKM measure is inconsistent among samples. *Theory Biosci*. 131(4):281–285.
Wagner MM, Campbell RG, Boudreau CA, Durbin EG. 2001. Nucleic acids and growth of *Calanus finmarchicus* in the laboratory under

different food and temperature conditions. *Mar Ecol Prog Ser*. 221:185–197.

Wallau GL, Capy P, Loreto E, Le Rouzic A, Hua-Van A. 2016. VHICA, a new method to discriminate between vertical and horizontal transposon transfer: application to the mariner family within Drosophila. *Mol Biol Evol*. 33(4):1094–1109.

Welch JJ, Bininda-Emonds OR, Bromham L. 2008. Correlates of substitution rate variation in mammalian protein-coding sequences. *BMC Evol Biol*. 8:53.

Wojewodzic MW, Rachamim T, Andersen T, Leinaas HP, Hessen DO. 2011. Effect of temperature and dietary elemental composition on RNA/protein ratio in a rotifer. *Funct Ecol*. 25(5):1154–1160.

Wolfe KH, Sharp PM, Li WH. 1989. Mutation rates differ among regions of the mammalian genome. *Nature* 337(6204):283–285.

Wright F. 1990. The 'effective number of codons' used in a gene. *Gene* 87(1):23–29.

Wu Y, Wang H, Hadly EA. 2017. Invasion of ancestral mammals into dim-light environments inferred from adaptive evolution of the phototransduction genes. *Sci Rep*. 7:46542.

Xing W, Shi Q, Liu H, Liu G. 2016. Growth rate, protein: rNA ratio and stoichiometric homeostasis of submerged macrophytes under eutrophication stress. *Knowl Manage Aquat Ecosyst*. 417:25.

Yang Z. 2007. PAML 4: phylogenetic analysis by maximum likelihood. *Mol Biol Evol*. 24(8):1586–1591.